Computational Studies of Aliphatic Alcohol Acidity

Robert Damrauer

Contribution from the Chemistry Department, University of Colorado at Denver, Denver, Colorado 80217-3364

Received February 24, 2000

Abstract: Computational studies have been used to examine the structural and energetic effects of adding small numbers of water molecules to methanol, *tert*-butyl alcohol, methoxide, and *tert*-butoxide. The effective fragment potential as well as Hartree−Fock methods reveals distinct structural effects with as few as two to four water molecules. Structural and energetic effects are used to probe the acidity reversal of simple aliphatic alcohols on going from the gas phase to protic solvents. Although the effective fragment potential and Hartree−Fock methods without sufficient electron correlation underestimate the number of water molecules that give rise to acidity reversal, the trend toward reversal is evident with small numbers of waters in all methods.

Introduction

Groundbreaking studies of the gas-phase acidities of aliphatic alcohols by Brauman and Blair in the late 1960s and early 1970s established that the order of gas-phase acidity of simple aliphatic alcohols is reversed from that in protic solvents.[1,2] Until then, it was widely held that the acidity order in protic solvents [$(CH_3$-OH > $(CH_3)_2$CHOH > $(CH_3)_3$COH] resulted either from inductive effects, with increasing numbers of electron-donating methyl substituents destabilizing the corresponding alkoxide ions, or from solvation effects in which the larger alkoxide ions were not solvated as effectively as smaller ones by protic solvents. Brauman and co-workers demonstrated that aliphatic groups such as methyl are not intrinsically electron donating, but rather affect gas-phase molecules because of their polarizability. Increasing the number and complexity of alkyl substituents in a regular molecular series in the gas phase can have the effect of stabilizing a negative charge and increasing acidity (the alcohols[1,2]) or of stabilizing a positive charge and increasing basicity (the amines[3]), both by mechanisms that are thought to be dominated by polarizability ($\approx 1/r^4$) effects. These early studies in gas-phase chemistry, because they exposed differences between the properties of molecules and their reactions in the gas and condensed phase, ushered in an explosion of gas-phase chemical studies.

Fundamental to an understanding of the reversal of aliphatic alcohol acidity in the gas phase and in protic solvents is detailed examination of the structure of protic solvents and their interactions with small molecules. This is a very active area of current research, both experimentally and computationally. Among many such studies are those examining small water clusters [$(H_2O)_n$],[4−12] water interacting with small molecules,[5,13−21] ion/water clusters,[22−36] and proton transfer.[37−39] In addition, the molecular details of solvation have begun to be elucidated in

(1) Brauman, J. I.; Blair, L. K. *J. Am. Chem. Soc.* **1968**, *90*, 6561−2.
(2) Brauman, J. I.; Blair, L. K. *J. Am. Chem. Soc.* **1970**, *92*, 5986−92.
(3) Brauman, J. I.; Riveros, J. M.; Blair, L. K. *J. Am. Chem. Soc.* **1971**, *93*, 3914−6.
(4) Liu, K.; Cruzan, J. D.; Saykally, R. J. *Science* **1996**, *271*, 929−33.
(5) Kim, K.; Jordan, K. D.; Zwier, T. S. *J. Am. Chem. Soc.* **1994**, *116*, 11568−9.
(6) Liu, K.; Loeser, J. G.; Elrod, M. J.; Host, B. C.; Rzepiela, J. A.; Pugliano, N.; Saykally, R. J. *J. Am. Chem. Soc.* **1994**, *116*, 3507−12.
(7) Wales, D. J.; Hodges, M. P. *Chem. Phys. Lett.* **1998**, *286*, 65−72.
(8) Bernal-Uruchurtu, M. I.; Ortega-Blake, I. *J. Phys. Chem. A* **1999**, *103*, 884−92.
(9) Jiang, J. C.; Chang, J.-C.; Wang, B.-C.; Lin, S. H.; Lee, Y. T.; Chang, H.-C. *Chem. Phys. Lett.* **1998**, *289*, 373−82.
(10) Pedulla, J. M.; Kim, K.; Jordan, K. D. *Chem. Phys. Lett.* **1998**, *291*, 78−84.
(11) Pedulla, J. M.; Vila, F.; Jordan, K. D. *J. Chem. Phys.* **1996**, *105*, 11091−9.
(12) Tsai, C. J.; Jordan, K. D. *J. Phys. Chem.* **1993**, *97*, 5208−10.
(13) Gruenloh, C. J.; Carney, J. R.; Arrington, C. A.; Zwier, T. S.; Fredericks, S. Y.; Jordan, K. D. *Science* **1997**, *276*, 1678−81.
(14) Pribble, R. N.; Zwier, T. S. *Faraday Discuss.* **1994**, *97*, 229−41.
(15) Pribble, R. N.; Zwier, T. S. *Science* **1994**, *265*, 75−9.
(16) Pribble, R. N.; Frost, R. K.; Hagemeister, F.; Zwier, T. S. *Proc. SPIE Int. Soc. Opt. Eng.* **1995**, *2548*, 136−46.
(17) Pribble, R. N.; Garrett, A. W.; Haber, K.; Zwier, T. S. *J. Chem. Phys.* **1995**, *103*, 531−44.
(18) Fredericks, S. Y.; Jordan, K. D.; Zwier, T. S. *J. Phys. Chem.* **1996**, *100*, 7810−21.
(19) Hagemeister, F. C.; Gruenloh, C. J.; Zwier, T. S. *Chem. Phys.* **1998**, *239*, 83−96.
(20) Gruenloh, C. J.; Carney, J. R.; Hagemeister, F. C.; Arrington, C. A.; Zwier, T. S.; Fredericks, S. Y.; Wood, J. T., III.; Jordan, K. D. *J. Chem. Phys.* **1998**, *109*, 6601−14.
(21) Carney, J. R.; Hagemeister, F. C.; Zwier, T. S. *J. Chem. Phys.* **1998**, *108*, 3379−82.
(22) Weis, P.; Kemper, P. R.; Bowers, M. T. *J. Am. Chem. Soc.* **1999**, *121*, 3531−2.
(23) Bryce, R. A.; Vincent, M. A.; Hillier, I. H. *J. Phys. Chem. A* **1999**, *103*, 4094−100.
(24) Woon, D. E.; Dunning, T. H., Jr. *J. Am. Chem. Soc.* **1995**, *117*, 1090−7.
(25) Petersen, C. P.; Gordon, M. S. *J. Phys. Chem. A* **1999**, *103*, 4162−6.
(26) Bewig, L.; Buck, U.; Rakowsky, S.; Reymann, M.; Steinbach, C. *J. Phys. Chem. A* **1998**, *102*, 1124−9.
(27) Cabarcos, O. M.; Weinheimer, C. J.; Lisy, J. M. *J. Chem. Phys.* **1998**, *108*, 5151−4.
(28) Berg, C.; Achatz, U.; Beyer, M.; Joos, S.; Albert, G.; Schindler, T.; Niedner-Schatteburg, G.; Bondybey, V. E. *Int. J. Mass Spectrosc. Ion Processes* **1997**, *167*/*168*, 723−34.
(29) Achatz, U.; Joos, S.; Berg, C.; Schindler, T.; Beyer, M.; Albert, G.; Niedner-Schatteburg, G.; Bondybey, V. E. *J. Am. Chem. Soc.* **1998**, *120*, 1876−82.
(30) Cheng, H.-P. *J. Phys. Chem. A* **1998**, *102*, 6201−4.
(31) Wang, Y.-S.; Chang, H.-C.; Jiang, J.-C.; Lin, S. H.; Lee, Y. T.; Chang, H.-C. *J. Am. Chem. Soc.* **1998**, *120*, 8777−88.
(32) Lehr, L.; Zanni, M. T.; Frischkorn, C.; Weinkauf, R.; Neumark, D. M. *Science* **1999**, *284*, 635−8.
(33) Ayotte, P.; Weddle, G. H.; Kim, J.; Johnson, M. A. *J. Am. Chem. Soc.* **1998**, *120*, 12361−2.
(34) Ayotte, P.; Weddle, G. H.; Johnson, M. A. *J. Chem. Phys.* **1999**, *110*, 7129−32.

10.1021/ja000678e CCC: $19.00
Published on Web 06/30/2000

studies of the dissolution of strong electrolytes such as HCl and NaCl in water, which reveal the importance of contact and solvent-separated ion pairs as dissociation occurs.[25,40] A study of the weak acid HF by Ando and Hynes also stresses the importance of contact and solvent-separated ion pairs, but, in addition, indicates that a barrier to contact ion pair formation is present.[39] Molecular details about weak electrolytes such as alcohols are more sparse, although specific computational studies by Silla and Geerlings and their respective co-workers dealing with the aliphatic alcohol acidity reversal have been carried out as have dynamic simulations of dilute alcohol solutions in water.[41−43] In one of these, MP4/6-31G(d) energy calculations (with sp diffuse functions on alcohol and alkoxide oxygen) give good agreement with experimental gas-phase acidities for CH_3OH, CH_3CH_2OH, $(CH_3)_2CHOH$, and $(CH_3)_3COH$. Bulk solvation effects are obtained by estimating the electrostatic and nonelectrostatic contributions to the solute−solvent interaction using the polarizable continuum model (PCM). By applying high-level molecular wave functions and suitable cavity sizes, this method reproduces the experimental trends nicely.[41] In work emphasizing the importance of group electronegativities and hardness, charge distributions are used as part of ab initio (6-31+G(d)) computations combined with the self-consistent isodensity polarizable continuum method (SCI−PCM) to demonstrate the reversal of alcohol acidities in the gas and aqueous phase.[42] In addition, recent studies by Huisken and co-workers have examined the vibrational spectroscopy of single methanol molecules in water clusters of various sizes (15−20).[44] Analysis of the C−O, C−H, and O−H stretching frequencies suggests that the methyl group points away from the "liquid" surface.

All continuum methods model solute−solvent interactions by treating the solvent as a bulk component whose dielectric properties affect the interactions. Although continuum methods vary in sophistication and have been quite successful in modeling the bulk behavior of solvents, their inherent deficiency is that they cannot probe solute−solvent or solvent−solvent molecular interactions.[45−47] Various computational methods can reveal these interactions, from costly ab initio quantum mechanical methods to less costly molecular mechanics methods. Each extreme has its advantages, depending on the size and nature of the system to be studied. Clearly, when large systems with many solvent interactions are to be studied, an ab initio treatment, while desirable, is practically impossible. As a result, a number of computational methods have been developed in which a quantum mechanical "core" interacts with a solvent that is variously modeled. Among the interacting solvent models are ones that are strictly molecular mechanical and ones that are more sophisticated, being based fundamentally in quantum mechanics. One such model is the effective fragment potential (EFP) method developed by Gordon and co-workers, where each solvent molecule is treated explicitly as a perturbation of the "core" Hamiltonian.[25,48−51] In the EFP model, the interaction between the quantum mechanical "core" (the active region in EFP parlance) and an individual solvent fragment is treated by adding one-electron potential terms to the active region Hamiltonian.

Since the most salient feature of computational methods such as the EFP model is their ability to provide information about individual solute−solvent and solvent−solvent interactions, examination of such interactions is expected to reveal important molecular details about solvation as well as additional information about properties and processes that differ in gas and condensed phase. Since the acidity reversal of aliphatic alcohols from gas phase to protic solvents is among the latter, particularly relevant questions surface for such a computational study of acidity reversal, namely: (1) what structural characteristics do the solvated alcohols and alkoxides display, (2) are there structural differences among these that could help explain the acidity reversal, (3) to what extent in structural terms can small numbers of protic solvent molecules be said to contribute to "bulk" solvent properties, and (4) how many protic solvent molecules are required for reversal? To address these questions, an EFP model study of methanol and *tert*-butyl alcohol acidity has been undertaken. These results, as well as relevant ab initio studies, are reported herein.

Computational Methods

A. Effective Fragment Potential Method. The EFP model developed by Gordon and co-workers has been described in detail and need be summarized only very briefly here.[25,48−51] The system is described by the Hamiltonian,

$$H = H_{AR} + V$$

in which H_{AR} is the ab initio Hamiltonian of the active region (the solutes being methanol, methoxide, tert-butanol, and tert-butoxide in this study) and V is the potential due to the solvent fragment (water in this study). In the current EFP formulation, V consists of one-electron terms that describe the (1) electrostatic (Coulombic), (2) polarization, and (3) exchange repulsion/charge-transfer interactions between solute and solvent and between solvent and solvent. Although the internal geometry of a water fragment is fixed in the EFP method, its relative position with respect to the solute is not. Implementation of the EFP method in the GAMESS suite of programs allows the use of analytical gradients for systems consisting of solute and fragment(s) as well as vibrational frequency analysis by means of numerical differences of the analytical gradients. Thus, geometric and energetic, as well as reaction path, information can be obtained for solute−fragment systems.

B. Computational Details. Calculations on methanol and *tert*-butyl alcohol and their corresponding alkoxides have been used to probe the alcohol reversal since these solutes not only show this behavior experimentally but are small enough to be amenable to high-level ab initio computation. Since the proton is a common feature in the alcohol dissociation ($ROH + (n+m)H_2O \rightarrow H^+(H_2O)_m + RO^-(H_2O)_n$), relative acidities can be obtained by ignoring the energy of the proton, whether bare or solvated. This assumes that $H^+(H_2O)_m$ is solvated to the same extent for methanol and *tert*-butyl alcohol. The fragment calculations have been carried out in the active alcohol region at the restricted Hartree−Fock (RHF) level of theory with the 6-31++G(d,p) basis set, while the water fragments have been modeled using the EFP method

(35) Ayotte, P.; Weddle, G. H.; Kim, J.; Kelley, J.; Johnson, M. A. *J. Phys. Chem. A* **1999**, *103*, 443−7.
(36) Dessent, C. E. H.; Kim, J.; Johnson, M. A. *Acc. Chem. Res.* **1998**, *31*, 527−34.
(37) Syage, J. A.; Steadman, J. *J. Phys. Chem.* **1992**, *96*, 9606−8.
(38) Tao, F.-M. *J. Chem. Phys.* **1998**, *108*, 193−202.
(39) Ando, K.; Hynes, J. T. *J. Phys. Chem. A* **1999**, *103*, 10398−408.
(40) Ando, K.; Hynes, J. T. *J. Phys. Chem. B* **1997**, *101*, 10464−78.
(41) Tunon, I.; Silla, E.; Pascual-Ahuir, J.-L. *J. Am. Chem. Soc.* **1993**, *115*, 2226−30.
(42) Safi, B.; Choho, K.; De Proft, F.; Geerlings, P. *J. Chem. Phys. A* **1998**, *102*, 5253−9.
(43) Fidler, J.; Rodger, P. M. *J. Phys. Chem. B* **1999**, *103*, 7695−705.
(44) Huisken, F.; Mohammad-Pooran, S.; Werhahn, O. *Chem. Phys.* **1998**, *239*, 11−22.
(45) Leach, A. R. *Molecular Modeling: Principles and Applications*, 1st ed.; Addison-Wesley Longman Limited: Essex, 1996.
(46) Gao, J. *Acc. Chem. Res.* **1996**, *29*, 289−305.
(47) Jensen, F. *Introduction to Computational Chemistry*; John Wiley & Sons: Chichester, 1999.
(48) Day, P. N.; Jensen, J. H.; Gordon, M. S.; Webb, S. P.; Stevens, W. J.; Krauss, M.; Garmer, D.; Basch, H.; Cohen, D. *J. Chem. Phys.* **1996**, *105*, 1968−86.
(49) Chen, W.; Gordon, M. S. *J. Chem. Phys.* **1996**, *105*, 11081−60.
(50) Webb, S. P.; Gordon, M. S. *J. Phys. Chem. A* **1999**, *103*, 1265−73.
(51) Merrill, G. N.; Gordon, M. S. *J. Phys. Chem. A* **1998**, *102*, 2650−7.

just described (hereafter abbreviated as the EFP method). This particular basis set was chosen as the largest that practically could be used for systems of the size studied. For each $ROH(H_2O)_n$ and $RO^-(H_2O)_n$ (R = CH_3 and $(CH_3)_3C$) (n = 0, 1, 2, 3, 4, 5, 6, 8, 10, and 14), full geometry optimizations (with the fixed fragment geometry restriction, vide supra) were carried out from various initial geometries.

As the number of fragment waters increases, the number of possible initial geometries also increases as does the number of optimized structures (in fact, dramatically so). When large numbers of structures were examined, it became clear that the potential energy surface for a given alcohol or alkoxide with a fixed number of fragments is quite flat. Numerical Hessians (matrix of energy second derivatives) of the lowest energy structures as well as others of similar energy were obtained from finite double differences of analytical derivatives and used to determine the nature of such structures (minima = positive definite Hessian; nth-order saddle point = n negative eigenvalues). The structures discussed herein all are minima whose vibrational analysis has been used to correct energies for zero point vibrational contributions (ZPC). These data are reported as enthalpies at 0 K. They have not been corrected for temperature effects, since the flat nature of the potential energy surfaces makes the normal rigid rotor−harmonic oscillator approximations for the entropy contributions suspect. Because the acidity values reported herein are ΔH_{acid} and because the computations have not been carried out with highly correlated wave functions, they are not expected to be accurate, although their relative values capture the acidity reversal trends. It is important to point out that many minima have been found with some of the larger water molecule species. Although their energies can vary by a few kilocalories (except in cases where the structural characteristics suggest that a particular species is not to be considered), using the lowest energy species gives the same acidity reversal results as either averaging or Boltzmann averaging. Clearly, there is no measure of whether the global minima have been found, which is why so many structures have been examined and why the analysis, comparing both averaged and lowest energy structures, has been carried out.

In addition to the EFP computations, a number of Hartree−Fock and second-order perturbation theory (MP2)[52] calculations have been carried out to evaluate the EFP model. Beginning with the lowest energy structures obtained from the EFP model studies, RHF optimizations using the 6-31++G(d,p) basis set have been carried out on $ROH(H_2O)_n$ and $RO^-(H_2O)_n$ (R = CH_3 and $(CH_3)_3C$) (n = 0, 1, 3, 5, and 6). MP2/6-311++G(d,p)//6-31++G(d,p) energies were obtained for $ROH(H_2O)_n$ and $RO^-(H_2O)_n$ (R = CH_3 and $(CH_3)_3C$) (n = 0, 1, 3, 5, and 6) using the optimized Hartree−Fock geometries as input. For n = 8, 10, and 14, the geometries from the EFP optimizations were used (hereafter abbreviated as the MP2 method). All computations were carried out using the GAMESS suite of programs.[53] MacMolPlot has been used to visualize the molecular structures.[54]

Results and Discussion

A. Structural Considerations: Methanol and *tert*-Butanol. The EFP optimized structures of methanol and *tert*-butyl alcohol, obtained at the RHF level of theory using the 6-31++G(d,p) basis set for the active region and the EFP method to describe the water fragments for n = 0, 1, 2, 3, 4, 5, 6, 8, 10, and 14 fragments, show quite interesting similarities as water fragments are added. A number of initial structures were optimized for each n value; a typical input structure for alcohol (ROH) optimization with n = 1−4 water fragments has the fragments arranged about the O−H bond, proximal to the H, with the fragment oxygens within hydrogen-bonding (H-bonding) distance of the H and the fragment hydrogen atoms directed away from the O−H bond and the hydrophobic (hydrocarbon) region.

Table 1. $ROH\cdots H_2O$ Distances as Function of Number of Coordinated Waters

no. of waters	EFP distances[a] (Å)	RHF distances[b] (Å)	difference (RHF − EFP)
	Methanol		
1	2.03	2.05	0.02
3	1.93	1.95	0.02
3	3.17	3.14	−0.03
3	3.59	3.58	−0.01
5	1.87	1.90	0.03
5	3.16	3.16	0.00
5	3.51	3.52	0.01
5	4.98	4.95	−0.03
5	5.46	5.46	0.00
6	1.80	1.84	0.04
6	3.22	3.20	−0.02
6	3.28	3.25	−0.03
6	3.60	3.63	0.03
6	3.82	3.84	0.02
6	4.04	4.02	−0.02
	tert-Butanol		
1	2.05	2.08	0.03
3	1.93	1.98	0.05
3	3.14	3.13	−0.01
3	3.56	3.59	0.03
5	2.06	2.10	0.04
5	3.08	3.11	0.03
5	3.62	3.72	0.10
5	3.71	3.77	0.06
5	5.32	5.40	0.08
6	1.85	1.92	0.07
6	3.08	3.08	0.00
6	3.35	3.37	0.02
6	3.40	3.44	0.04
6	3.71	3.72	0.01
6	4.86	4.84	−0.02

[a] Carried out at EFP/6-31++G(d,p). [b] Carried out at 6-31++G(d,p)//6-31++G(d,p).

For larger values of n, it is necessary to arrange all water fragments after the first four at a greater distance from the O−H bond, but otherwise their geometric relationship to the O−H bond is similar. The corresponding optimized structures have several common features: (1) the structures of methanol and *tert*-butyl alcohol in the active region are very similar, no matter how many water fragments are present (C−O bond distances in methanol and *tert*-butyl alcohol are 1.40−1.41 and 1.41−1.42 Å; C−H bond distances in methanol are 1.08−1.09 Å, and C−C bond distances are 1.53 Å for *tert*-butyl alcohol), (2) one water fragment is H-bonded to the O−H hydrogen ($ROH\cdots OH_2$ distances are 1.80−2.06 Å in Table 1), but as the number of water fragments increases, the number of H-bonds to the O−H oxygen increases to either one or two (vide infra), and (3) other water fragments are arranged in extended H-bonded networks (Figure 1). These characteristics of the optimized fragment structures obtain even when quite different input structures are used. The optimized RHF structures of methanol and *tert*-butyl alcohol show the same characteristics as the corresponding EFP structures (1−3 above) as waters are added (Table 1).

Analysis of the EFP and RHF structures indicates that as the number of water molecules in contact with methanol or *tert*-butyl alcohol increases, the complexity of the H-bonded network increases. This is not surprising, given the results of numerous experimental and computational studies that have examined water cluster [$(H_2O)_n$] structure.[4−12,55] It is well established that the lowest energy structures for n = 3−5 are cyclic and that

(52) Møller, C.; Plesset, M. S. *Phys. Rev.* **1934**, *46*, 618−22.
(53) Schmidt, M. W.; Baldridge, K. K.; Boatz, J. A.; Elbert, S. T.; Gordon, M. S.; Jensen, J. H.; Koseki, S.; Matsunaga, N.; Nguyen, K. A.; et al. *J. Comput. Chem.* **1993**, *14*, 1347−63.
(54) Bode, B. M.; Gordon, M. S. *J. Mol. Graphics* **1998**, *16*, 133−8.
(55) Liu, K.; Brown, M. G.; Carter, C.; Saykally, R. J.; Gregory, J. K.; Clary, D. C. *Nature* **1996**, *381*, 501−3.

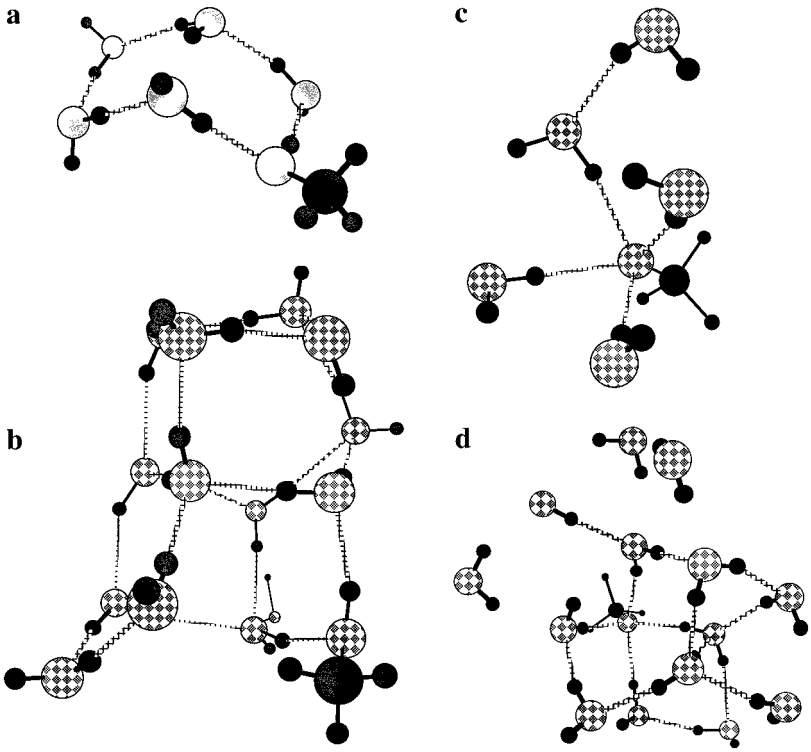

Figure 1. Typical methanol and methoxide fragment structures (for $n = 5$ and 14): (a) methanol with 5 fragments; (b) methanol with 14 fragments; (c) methoxide with 5 fragments; (d) methoxide with 14 fragments. Both methanol structures are oriented to show as clearly as possible hydrogen bonding to and among the water fragments. Hydrogen bonds are highlighted by crosshatched lines. The methoxide structures are oriented to emphasize (1) the $O^{-}\cdots H$ interaction with four water fragments (for $n = 5$) and (2) the general complexity of the larger water network (for $n = 14$). Hydrogen bonds are highlighted by crosshatched lines.

larger n values give rise to more structural possibilities. Thus, the first "three-dimensional" structures obtain when $n = 6$, where several low-energy structures have been reported.[10] Although the cage structure is very likely the global minimum, prism, cyclic, book, and boat structures are low-energy species as well.[4−12,55] What distinguishes the more complex from the cyclic structures is the number of H-bonds that the water molecules make. In cyclic structures, each water contributes only one H-bond (i.e., only one hydrogen atom is an H-bond donor), while in more complex structures, some water molecules make two H-bonds (i.e., both hydrogen atoms are H-bond donors). For the $n = 6$ cage structure, two waters are doubly H-bonded; in the prism structure, three waters are doubly H-bonded; in the cyclic structure, each water is singly H-bonded.

Examination of the EFP and RHF structures reveals similar trends (see Figure 1 for some representative EFP structures) (Table 2) (≤2.1 Å is considered to be the H-bond distance). *tert*-Butyl alcohol has a cyclic structure when $n = 2$, while that of methanol is close to cyclic. Structures of methanol and *tert*-butyl alcohol having three fragments are cyclic. These structures are similar to methanol−water clusters with two and three waters studied with small basis sets.[56] Both methanol and *tert*-butyl alcohol with five waters have structures analogous to those of the low-energy book structure of the water hexamer (Figure 1), where the alcohol OH takes the place of a water. The structure for *tert*-butyl alcohol having only four bound waters has a doubly H-bonded water, although not until six waters are coordinated to methanol are individual water molecules doubly H-bonded. Some water molecules in the structures studied make no H-bonds through their hydrogen atoms, although they are H-bonded to other water molecules through their oxygen atom (i.e., they are H-bond acceptors, but not donors). Only slight differences occur between the EFP and RHF structures in terms of H-bonding. The most telling feature of these structures is that the water molecules H-bond among themselves "building" toward a bulk water structure. The "off to one side" feature of

Table 2. Number of H−Bonded Waters (H-Bonding Distance ≤ 2.1 Å)

species CH_3OH $n H_2O$ (n)	no. of water fragment molecules: making zero H-bonds	making one H-bond	making two H-bonds
	Methanol		
1	1 (1)	0	0
2	1	1	0
3	1 (1)	2 (2)	0 (0)
4	1	3	0
5	1 (1)	4 (4)	0 (0)
6	2 (2)	2 (4)	2 (0)
8	0	7	1
10	1	7	2
14	2	5	7

species $(CH_3)_3COH$ $n H_2O$ (n)	no. of water fragment molecules: making zero H-bonds	making one H-bond	making two H-bonds
	tert-Butanol		
1	1 (1)	0	0
2	1	1	0
3	1 (1)	2 (2)	0 (0)
4	1	2	1
5	0 (0)	5 (5)	0 (0)
6	1 (1)	5 (5)	0 (0)
8	1	5	2
10	1	7	2
14	0	8	6

[a] RHF results in parentheses.

(56) Williams, R. W.; Cheh, J. L.; Lowrey, A. H.; Weir, A. F. *J. Phys. Chem.* **1995**, *99*, 5299−307.

Table 3. Representative Methoxide and *tert*-Butoxide Bond Distances

no. of waters	bond length (Å)			
	EFP[a] C−O	RHF[b] C−O	av EFP C−H	av RHF C−H
	Methoxide			
0	1.33	1.33	1.12	1.12
1	1.34	1.34	1.12	1.11
3	1.35	1.36	1.11	1.10
5	1.36	1.37	1.10	1.10
6	1.37	1.37	1.10	1.10
8	1.37		1.10	
10	1.37		1.10	
14	1.37		1.10	

no. of waters	bond length (Å)			
	EFP[a] C−O	RHF[b] C−O	av EFP C−C	av RHF C−C
	tert-Butoxide			
0	1.34	1.34	1.56	1.56
1	1.34	1.35	1.55	1.55
3	1.36	1.36	1.54	1.54
5	1.37	1.38	1.54	1.54
6	1.37	1.38	1.54	1.54
8	1.38		1.54	
10	1.38		1.54	
14	1.38		1.54	

[a] Carried out at EFP/6-31++G(d,p). [b] Carried out at 6-31++G(d,p)//6-31++G(d,p).

H-bonded networks that is evident in Figure 1 is best explained in steric terms, where the extending bulk water structures avoid interactions with the methyl or *tert*-butyl groups of the alcohols.

Recent molecular dynamic (MD) studies of a series of aqueous alcohols are consistent with the structural effects presented here.[43] These MD simulations suggest that dilute alcohol concentrations have little effect on the overall water structural network but that alcohol−water H-bonding occurs in the O−H region with some disruption of the water structure in that region. No evidence was found for special water interactions (structural disruption) in the hydrophobic region of the alcohols. Although the dynamic behavior of water varied as a function of alcohol structure, this was not attributed to variations in H-bonding strength.

Methoxide and *tert*-Butoxide. The EFP and RHF optimized structures of methoxide and *tert*-butoxide are quite similar, although in contrast to the alcohols, the C−O bonds of the alkoxides lengthen ∼0.04 Å in going from 0 to 14 water fragments. Most of the C−O bond lengthening occurs as the first six waters are added for methoxide, but the *tert*-butoxide C−O bond lengthens another 0.01 Å going from 6 to 14 water fragments (Table 3). The RHF results are similar, with C−O bond lengthening of ∼0.04 Å with six water additions for both alkoxides. The C−H bonds in methoxide and the C−C bonds in *tert*-butoxide shorten ∼0.02 Å as waters are added in both the EFP and RHF studies. The lengthening of the alkoxide C−O bonds as more waters are added reflects the fundamental difference between gas- and the aqueous-phase behavior. A shorter C−O bond in the gas phase results because there is no medium effect to stabilize the charge (a smaller bond dipole results), while the longer C−O bond as more waters coordinate results because of the stabilizing interactions with the polar medium.[57,58]

The alkoxide−water structures show that up to four water molecules can surround the alkoxide oxygen (ion−dipole interaction); typically one hydrogen atom of each of the four waters is within 2 Å (Figure 1 and Table 4). The other hydrogen points outward and is H-bonded to other water molecules that are arranged in shell-like H-bonded networks. The networks extend outward, avoiding the hydrophobic portion of the alkoxides (Figure 1). There are greater differences between the EFP and RHF alkoxide structures than the alcohols, no matter how many waters are considered (up to six). In virtually every comparison, the closest distance from the negatively charged alkoxide oxygen to the coordinated hydrogen of water ($RO^-\cdots HOH$) is shorter for the RHF structures (0.10 Å for methoxide and 0.06 Å for *tert*-butoxide) (Table 4). This is not surprising, given that the EFP method also overestimates the Na^+-O bond length in sodium chloride−water clusters, since the EFP model potential is designed for weak, H-bond-like interactions, not for stronger ion−dipole interactions.[25]

Table 4. Closest Water $RO^-\cdots H_2O$ Distances (Å) as Function of Number of Coordinated Waters

no. of waters	EFP distances[a]	RHF distances[b]	difference (RHF − EFP)
	Methoxide		
1	1.79	1.61	−0.18
3	1.87	1.75	−0.12
3	1.87	1.75	−0.12
3	1.87	1.75	−0.12
5	1.85	1.76	−0.09
5	1.86	1.79	−0.07
5	1.90	1.80	−0.10
5	1.90	1.82	−0.08
5	3.94	3.81	−0.13
6	1.78	1.69	−0.09
6	1.86	1.76	−0.10
6	1.92	1.88	−0.04
6	1.94	1.89	−0.05
6	3.49	3.36	−0.13
6	3.99	3.94	−0.05
	tert-Butoxide		
1	1.80	1.66	−0.14
3	1.88	1.79	−0.09
3	1.88	1.79	−0.09
3	1.88	1.79	−0.09
5	1.85	1.76	−0.09
5	1.90	1.87	−0.03
5	1.92	1.89	−0.03
5	1.95	1.90	−0.05
5	3.92	3.93	0.01
6	1.82	1.73	−0.09
6	1.90	1.85	−0.05
6	1.96	1.93	−0.03
6	1.98	1.93	−0.05
6	3.57	3.46	−0.11
6	3.88	3.84	−0.04

[a] carried out at EFP/6-31++G(d,p). [b] carried out at 6-31++G(d,p)//6-31++G(d,p).

B. Acidity Reversal: Variation of Number of Waters. Table 5 presents the relative ZPC energies of $CH_3OH(H_2O)_n$, $CH_3O^-(H_2O)_n$, $(CH_3)_3COH(H_2O)_n$, and $(CH_3)_3CO^-(H_2O)_n$ for $n = 0$, 1, 2, 3, 4, 5, 6, 8, 10, and 14 fragments obtained by the EFP method. These data are the lowest relative energy values found for each n (see Computational Methods for further details). Also given in Table 5 are the ΔH_{acid} values obtained from the lowest energy species. Examination of these data lead to several conclusions: (1) the relative energies of all species decrease as the number of water fragments increases (that is, methanol·1 water relative to methanol or methoxide·1 water relative to methoxide, etc.), (2) the decrease in the relative energies of the alcohols is smaller per added water fragment than that of the alkoxides, (3) the relative energies of methanol and *tert*-butyl alcohol decrease linearly as water fragments are

(57) Wong, M. W.; Frisch, M. J.; Wiberg, K. B. *J. Am. Chem. Soc*. **1991**, *113*, 4776−82.
(58) Wiberg, K. B. *J. Am. Chem. Soc.* **1990**, *112*, 3379−85.

Table 5. Relative Energy Data from EFP Computations and Acidities from EFP, RHF, and MP2 Studies

species CH_3OH nH_2O (n)	relative ZPC energy (kcal/mol) methanol EFP[a,b]	relative ZPC energy (kcal/mol) methoxide EFP[a,b]	acidity (kcal/mol) EFP[a]	acidity (kcal/mol) RHF[c]	acidity (kcal/mol) MP2[d]
		Methanol/Methoxide			
0	0.0	0.0	389	389	392
1	−3.3	−16	376	372	373
2	−9.2	−31	367		
3	−16	−46	359	355	355
4	−21	−58	352		
5	−28	−67	350	346	344
6	−36	−76	349	344	344
8	−48	−93	344		347
10	−60	−107	342		342
14	−83	−135	337		338

species $(CH)_3COH$ nH_2O (n)	relative ZPC energy (kcal/mol) *tert*-butyl alcohol EFP[a,b]	relative ZPC energy (kcal/mol) *tert*-butoxide EFP[a,b]	acidity (kcal/mol) EFP[a]	acidity (kcal/mol) RHF[c]	acidity (kcal/mol) MP2[d]
		tert-Butanol/*tert*-Butoxide			
0	0.0	0.0	384	384	383
1	−3.6	−15	372	369	367
2	−9.9	−30	364		
3	−18	−44	358	354	353
4	−22	−55	351		
5	−28	−64	348	345	342
6	−37	−73	348	345	340
8	−49	−86	347		342
10	−64	−105	342		340
14	−88	−133	339		334

[a] Carried out at EFP/6-31++G(d,p). [b] Relative to −114.997 53 Hartree for methanol, −114.377 95 for methoxide, −232.035 84 for *tert*-butyl alcohol, and −231.424 02 for *tert*-butoxide (zero point corrected). [c] Carried out at 6-31++G(d,p)//6-31++G(d,p). [d] Carried out at MP2/6-311++G(d,p)//6-31++G(d,p).

added with the relative energy of *tert*-butyl alcohol decreasing as a function of added water more than that of methanol (linear regression, $R^2 = 0.998$ for both methanol and *tert*-butyl alcohol), and (4) the relative energies of methoxide and *tert*-butoxide decrease nonlinearly as water fragments are added with the relative energy of methoxide decreasing as a function of added water more that of *tert*-butoxide. In addition, the ΔH_{acid} values show the acidity reversal with *tert*-butyl alcohol being the stronger acid in the gas phase and methanol, in water.

When the relative energies of the alcohols and alkoxides as a function of added waters are compared with the structural characteristics of these species, there is an interesting break in the relative solvation energies for both the alcohols and alkoxides near where the structural data indicate that the water network begins to grow. Thus, addition of the first water fragment lowers the energy of both alcohols by 3−4 kcal/mol; all other water fragment additions lower the energy by 6−8 kcal/mol. The corresponding structural effect on the alcohols shows that the first water makes its H-bond with ROH, but further water fragment additions contribute predominantly to the water structural network. For the alkoxides, there is a distinct change in the energetic effect of adding a water fragment after three have been added (the first three lower the energy 14−16 kcal/mol; the fourth, ∼11 kcal/mol; all others, 6−9 kcal/mol). This corresponds with the structural effect of the alkoxides having a maximum of four water molecules interacting with the negative charge of RO^-. Although these data also show an acidity crossover occurring near where six water fragments have been added (Figure 2), examining the structural relationships of incrementally adding water molecules using the EFP or RHF methods reveals no unusual features arising when six waters have been added. Indeed, both alcohols and alkoxides have

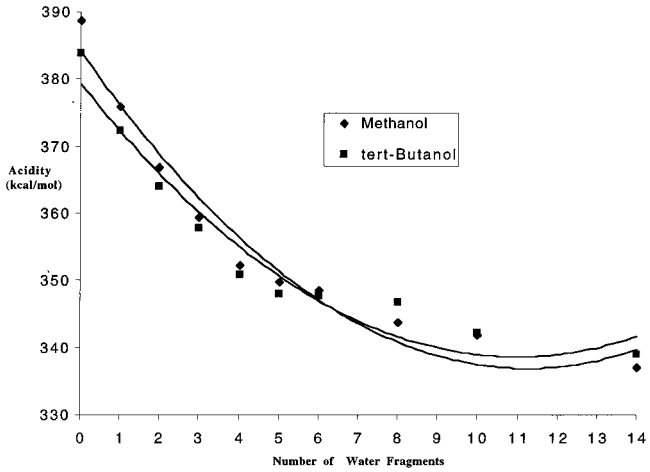

Figure 2. Acidity (determined at EFP//6-31++G(d,p)) versus number of water fragments.

adopted their characteristic structural features when as few as two to four water molecules have been added.

Surprisingly, the EFP results suggest that the acidity reversal is more dependent on the relative energy change of methanol versus *tert*-butyl alcohol than on their corresponding alkoxides. Examination of Table 5 suggests that as the number of water fragments increases the energy difference between methanol and *tert*-butyl alcohol increases. These data suggest that *tert*-butyl alcohol is better stabilized by adding water fragments than methanol. The EFP energy difference variation between methoxide and *tert*-butoxide is much smaller, although, as might be expected, the relative energy lowering is slightly greater for methoxide for all values of n. Thus, although each water fragment addition has a larger absolute energy effect on the alkoxides than the alcohols, the divergence in the relative energies of the alcohols has a greater effect on the acidity reversal; this issue will be revisited below. Because the EFP relative energy data alone show the acidity reversal, this suggests that entropy considerations are of minor importance (note: estimates of entropy effects in the vibrational analyses are not valid because of the flat nature of the potential energy surface—see Computational Methods). Silla and co-workers have addressed this in their study of the differences in gas-phase acidities of these aliphatic alcohols and concluded "that the differences in the gas-phase deprotonation free energies of the alcohols ... are mainly due to differences in internal energy".[41]

Acidities obtained from the zero point corrected RHF energies of $CH_3OH(H_2O)_n$, $CH_3O^-(H_2O)_n$, $(CH_3)_3COH(H_2O)_n$, and $(CH_3)_3CO^-(H_2O)_n$ for $n = 0$, 1, 3, 5, and 6 also are presented in Table 5. The RHF and EFP results show the same acidity reversal trends, thus providing another example of how closely the EFP model follows energy trends of the RHF calculations (Figure 3). Nevertheless, the RHF and EFP results differ in terms of the relative energies of methanol and *tert*-butyl alcohol with added water molecules. The RHF data show that the relative energies of the alcohols are within 2 kcal/mol and vary in no regular way, while the relative energies of the alkoxides diverge linearly as waters are added, with methoxide being more stabilized than *tert*-butoxide (linear regression of the alkoxides adding waters, $R^2 = 0.980$). These results suggest in a more intuitive way that the acidity reversal is largely a matter of the increasing stabilization of methoxide as waters are added, a result that others have observed.[41,42]

Finally, acidities obtained from single point MP2/6-311++G(d,p) computations (Table 5), which have been carried out on structures obtained from RHF optimizations ($n = 0$, 1, 3, 5,

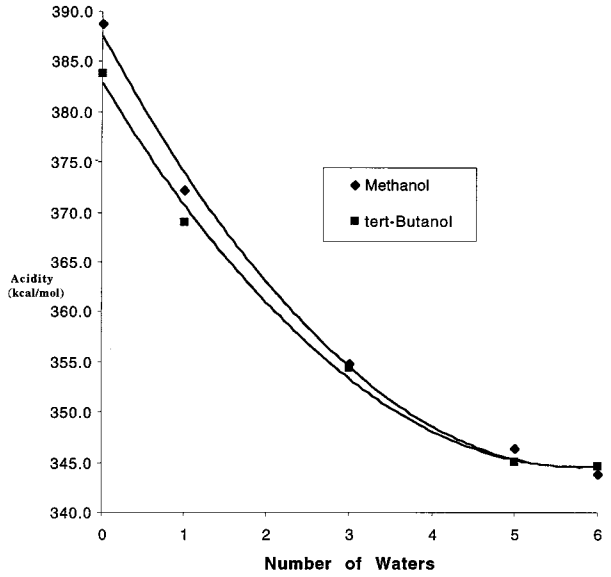

Figure 3. Acidity (determined at 6-31++G(d,p))//6-31++G(d,p)) versus number of water molecules.

and 6) and structures obtained from EFP optimizations ($n = 8$, 10, and 14), show some narrowing of the gap between the gas phase and water acidities of methanol and *tert*-butyl alcohol, but not a pronounced one. Although these are higher level computations, they are not strictly comparable with those previously discussed because complete MP2 optimizations are impractical for systems of this size. Despite this, the MP2 data suggest that the EFP and RHF calculations, because they use uncorrelated wave functions, give an exaggerated picture of the number of solvent molecules that are necessary for acidity reversal. Nevertheless, it seems clear that a relatively small number of coordinated water molecules is sufficient to bring about acidity reversal. Although the number is clearly not as small as six, it is likely that the effect is predominantly enthalpic in nature and that enthalpy effects are more important for the aquated alkoxides than the alcohols. It is notable that this is evident in both the reported structural and energy effects.

Concluding Remarks

The EFP, RHF, and MP2 methods have been used to examine the structural and energetic effects of adding individual water molecules in the vicinity of methanol, *tert*-butyl alcohol, methoxide, and *tert*-butoxide as a way probing the acidity reversal of simple aliphatic alcohols on going from the gas phase to protic solvents. The structures of methanol and *tert*-butyl alcohol as water molecules are added are dominated by a water H-bonding to the O−H hydrogen and a structural network of additional waters that can H-bond to the O−H oxygen as well as develop a "bulk" water structure, which is characterized by an increasing importance of doubly H-bonded waters. As water molecules surround methoxide, and *tert*-butoxide, the structural motif becomes dominated by four waters coordinated to the negative oxygen.

All three computational methods suggest that the acidity reversal of these alcohols is a subtle feature that depends on small differences between alcohol and alkoxide energies. Both the EFP and RHF methods indicate that as few as six waters are enough to model the acidity reversal. The MP2 calculations give some acidity narrowing with a few added waters. While clearly it is artificial to examine the energy effects of a few hydrated waters, it is important to emphasize that the energy trends, expressed more in the alkoxides than the alcohols, are already evident with a few waters of hydration using both the EFP and ab initio methods. Moreover, important structural features are revealed in these studies, where clear indications of the nature of the important interactions among hydrating waters and the alcohols and alkoxides are seen.

Acknowledgment. This work has been supported by the Research Corp. through a Cottrell College Science Award and by the Petroleum Research Fund, administered by the American Chemical Society. Particular thanks go to Professor Mark S. Gordon for many helpful discussions and for encouragement, support, and hospitality during a sabbatical visit at Iowa State University. His research group provided a comfortable atmosphere in which to work as well a great deal of technical help. Thanks particularly go to Michael Schmidt, whose insights in GAMESS taught me a great deal. Finally, the more demanding MP2 calculations (*tert*-butyl alcohol and *tert*-butoxide with $n = 14$) were performed on the SP2 at the Maui High Performance Computation Center and on the ERDC T3E. This computer time was made available through a DOD Grand Challenge Grant to Professor Mark Gordon and is gratefully acknowledged.

Supporting Information Available: Tables containing absolute and relative energies for the EFP, RHF, and MP2 calculations as well as optimized Cartesian coordinates for the EFP structures can be found in the Supporting Information, which is available free of charge via the Internet at http://pubs.acs.org.

JA000678E